Progress in the understanding of edge transport in the Quasi-Continuous Exhaust regime on TCV

B. Labit[1], P. Hennequin[2], S. Rienäcker[2], Y. Wang[1], M. van Rossem[1], M. La Matina[3,4], C. Wüthrich[1], M. Dunne[5], M. Faitsch[5], O. Sauter[1], E. Viezzer[6]

the TCV Team[*] and the EUROfusion Tokamak Exploitation team[†]

[1]*Swiss Plasma Center (SPC), Ecole Polytechnique Fédérale de Lausanne (EPFL), CH-1015 Lausanne, Switzerland,* [2]*Laboratoire de Physique des Plasmas (LPP), CNRS, Sorbonne Université, Ecole polytechnique, Institut Polytechnique de Paris, Palaiseau, France,* [3]*Consorzio RFX, C.so Stati Uniti 4, 35127 Padova, Italy,* [4]*CRF - University of Padova, Italy,* [5]*Max-Planck-Institute for Plasma Physics, Boltzmannstr. 2, D-85748 Garching, Germany,* [6]*Department of Atomic, Molecular and Nuclear Physics, University of Seville, Seville, Spain*

Introduction – The Quasi-Continuous Exhaust (QCE) regime is an attractive scenario not only for a fusion reactor but also for ITER or JT-60SA. Indeed this scenario features many of the confinement and exhaust parameters required in future tokamaks (f_G, β_N, H_{98y2},...) [1]. Within EUROfusion experimental programme, the QCE has been established and investigated in AUG [2], TCV [3] and JET [4]. By achieving the QCE on JET, including in D-T operation, the parameter space for QCE has been extended to lower collisionalities giving confidence for an extrapolation to next step devices [5]. This contribution reports on the progress made in the physics understanding of the QCE regime in TCV.

Pedestal analysis – The recipe to achieve QCE is relatively simple: a sufficient density at the separatrix and a strong plasma shaping. In Fig. 1, the temparature and density pedestal profiles for a type-I (#61057, black) and a QCE (#61056, red) are presented. The only difference between both shots is the larger triangularity for #61056 (see [3] for details). While the temperature profile is almost unchanged between both shots, the separatrix density is increased for the QCE case ($\frac{n_{e,sep}}{n_G} \sim 0.08 \rightarrow \sim 0.15$) leading to a reductiion of the pedestal density gradient. These observations suggest that an additional transport mechanism is triggered and sufficiently weak to not destroy the pedestal but sufficiently strong to avoid steep pressure gradients and ELMs. As proposed in [6], ballooning modes might be destabilised at the pedestal foot due to a reduction of the local magnetic shear. We analysed the stability to ∞-n ballooning modes for both pedestals and the results are reported in Fig.2, where the stability boundaries are plotted together with the experimental points for three different positions. A strking difference is observed at the pedestal foot ($\rho_\psi = 0.99$): the stability boundary is strongly affected by the

[*]*See author list of "B.P. Duval 2024 Nucl. Fusion **62** 042018"*

[†]*See author list of "E. Joffrin et al 2024 Nucl. Fusion **62** 042018"*

increased shaping and is now close to the experimental point, suggesting a contribution to turbulent transport from ballooning modes. In the next section, experimental results are reported to characterize fluctuations inside the pedestal.

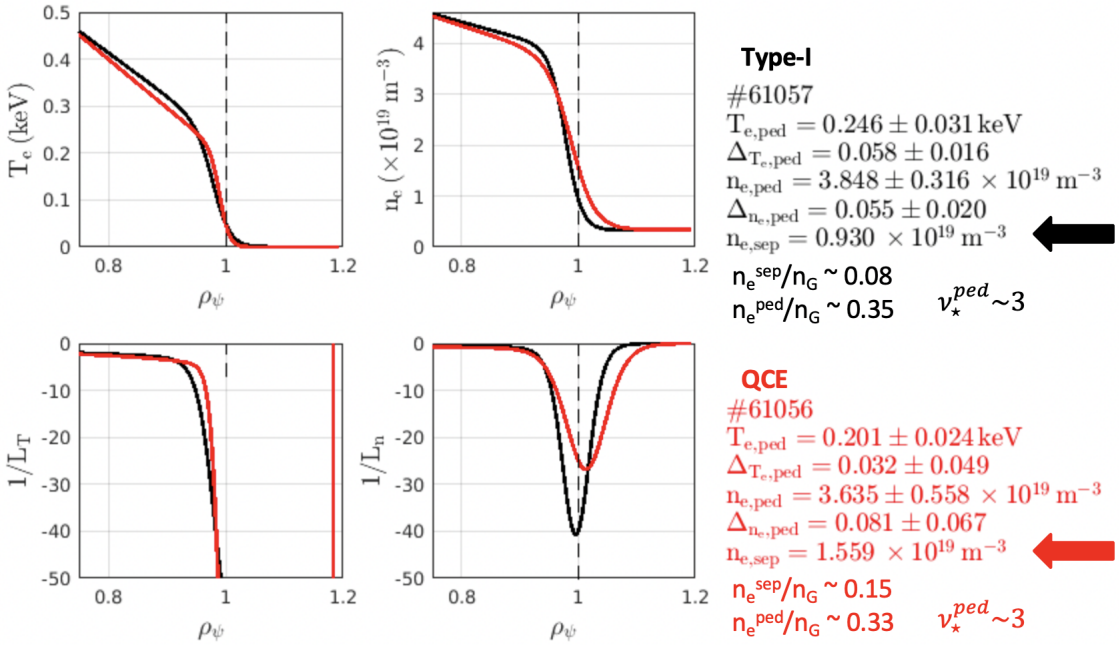

Figure 1: *Kinetic pedestal profiles and their gradients for Type-I (black) and QCE (red). The main difference is a reduced density gradient for QCE suggesting an additional transport mechanism.*

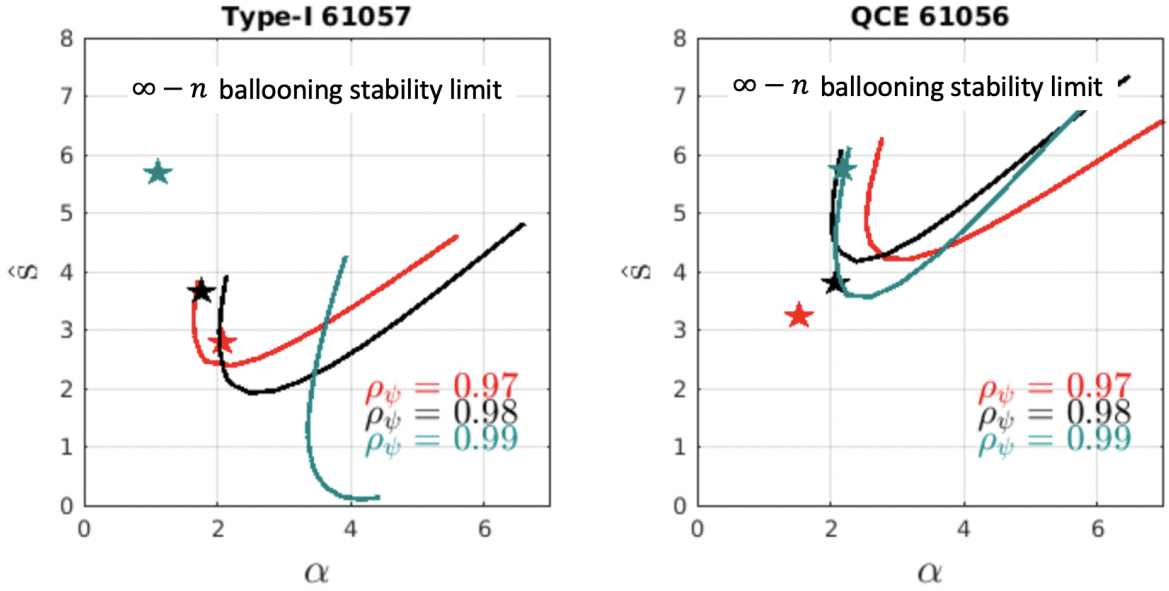

Figure 2: *Stability analysis for ∞-n ballooning modes for Type-I (left) and QCE (right).*

Experimental setup – TCV is equipped with several turbulence diagnostics. A short pulse reflectometer [7] and a Doppler backscattering system [8] share the same port and transmission lines, so can't be used at the same time. Similarly a thermal helium beam diagnostic [9] and a gas puff imaging system [10] are sharing the same port and optics. The same QCE plasma (170 kA/1.4 T/$q_{95} \sim 4.7$) has been repeated in order to get all possible combinations

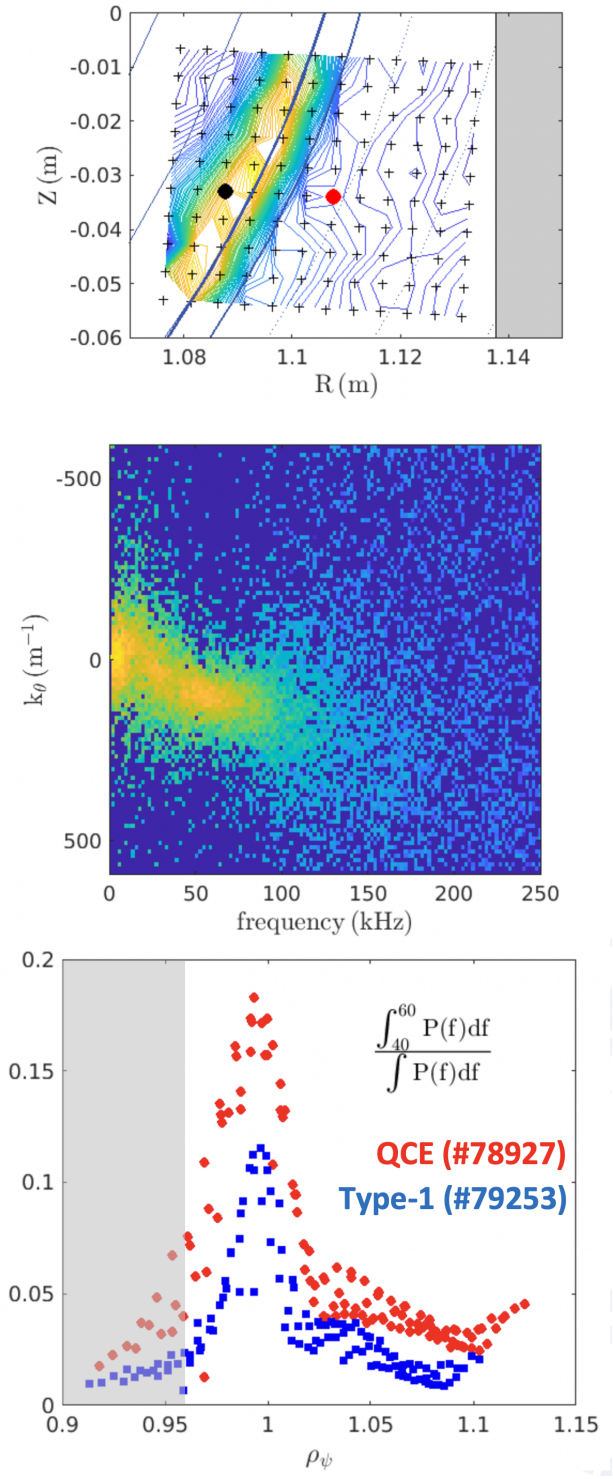

Figure 3: *Spectral analysis of GPI data for QCE shot #78927 – top) 2D map of the energy content in the frequency range 40-60 kHz – middle) statistical dispersion relation from which k_θ is inferred – bottom) Comparison with Type-I case (#79253).*

of measurements (GPI & SPR, GPI & DBS, ...). In the following, we are focusing on the GPI results.

Spectral analysis – The GPI diagnostics measures the line radiation intensity I from excited neutral atoms of helium. It consists in an array of 12×10 pixels (6 × 5 cm) sampled at 1 GHz (Fig. 3, top). For quantitative analysis, a normalised intensity $\tilde{I}$ is defined as follows $\tilde{I} = \frac{I - \langle I \rangle_{1ms}}{\langle I \rangle_{1ms}}$ where $\langle I \rangle_{1ms}$ is the moving average. The power spectral density $\mathscr{P}(f)$ was computed for $\tilde{I}$ measured inside the separatrix (black dot in Fig. 3, top) and in the SOL (red dot in Fig. 3, top) for QCE shot #78927. While the spectrum from the SOL is broadband, the one from the edge features a coherent mode at $\sim$ 50 kHz. To assess the localisation and the intensity of the coherent mode, the quantity $\frac{\int_{40kHz}^{60kHz} \mathscr{P}(f)}{\int_{0}^{500kHz} \mathscr{P}(f)}$ was computed and plotted in Fig. 3, top). It is clearly visible that the coherent mode is localised inside the separatrix. Note that below $\rho_\psi < 0.95$, the SNR of GPI is strongly reduced, so it can't be concluded if the mode extends further inside. A similar analysis from DBS seems to suggest it is the case (not shown).

As a next step, we tried to evaluate the poloidal wavenumber k_θ of this coherent mode. To do so, the statistical dispersion relation was computed (shown in Fig 3, middle) [11] based on the cross-phase shift between adjacent pixels in the poloidal direction. It is found that $k_\theta \sim 100 m^{-1}$ which gives an estimate for the poloidal mode number $m \sim$ 30. Another estimate from the DBS gives $k_\perp$ (which

is not exactly k_θ) of the order of 140 m^{-1} (not shown).

GPI data have been also collected for a type-I ELM plasma (#79253). A similar spectral analysis for $\tilde{I}$ has been done and the results are shown in Fig. 3, bottom). It is observed that the energy content in the frequency range 40-60 kHz is reduced compared to the QCE regime, not only inside the separatrix but also in the SOL, which might indicate a reduced transport at the pedestal foot as suggested by MHD previous analysis.

Outlook – The quasi-continuous exhaust (QCE) regime is a well established regime in EU tokamaks (AUG, TCV and JET) and its physical understanding is progressing well. The MHD analysis of TCV QCE pedestals supports the interpretation proposed by AUG for QCE access: increased transport from ballooning modes at the pedestal foot reduces density gradients and prevents the occurence of large ELMs. Turbulence data, collected with various diagnostics, shows a weakly coherent mode (50 kHz) inside the separatrix for QCE plasmas on TCV which might be the additional transport mechanism needed to reach QCE.

Since the transport in the SOL is increased for QCE plamas, SOL density profiles tends to flatten (density shoulder) and the interaction with the first wall increases. So, it is important to quantify and understand the heat and particle loads on the first wall, since it could be a potential limitation for the extrapolation of the QCE regime. Finally the turbulence characterisation for type-I and for other ELM-free regimes observed in TCV (X-Point Radiator and Negative Triangularity) will be extended.

Acknowledgements – This work has been carried out within the framework of the EUROfusion Consortium, partially funded by the European Union via the Euratom Research and Training Programme (Grant Agreement No 101052200 – EUROfusion). The Swiss contribution to this work has been funded by the Swiss State Secretariat for Education, Research and Innovation (SERI). Views and opinions expressed are however those of the author(s) only and do not necessarily reflect those of the European Union, the European Commission or SERI. Neither the European Union nor the European Commission nor SERI can be held responsible for them. This work was supported in part by the Swiss National Science Foundation.

References

[1] E. Viezzer et al, Nuclear Materials and Energy 34 (2023) 101308
[2] M. Faitsch et al, Nucl. Fusion 63 (2023) 076013
[3] B. Labit et al, Nucl. Fusion 59 (2019) 086020 50
[4] M. Faitsch et al, Nucl. Fusion 65 (2025) 024003
[5] M. Dunne et al, The physics of ELM-free regimes in EUROfusion tokamaks, 30th IAEA Fusion Energy Conference (FEC2025)
[6] L. Radovanovic et al, Nucl. Fusion 62 (2022) 086004
[7] P. Molina Cabrera, Rev. Sci. Instrum. 90 (2019) 123501
[8] S Rienäcker et al, Plasma Phys. Control. Fusion 67 (2025) 065003
[9] M. Ugoletti et al, Rev. Sci. Instrum. 95, (2024) 083530
[10] N. Offeddu et al, Rev. Sci. Instrum. 93, (2022) 123504
[11] FM Poli, *Electrostatic instabilities and turbulence in a toroidal magnetized plasma*, EPFL thesis 3849 (2007)